Synthesis and stability of amorphous $Cu_{60}Ti_{40-x}Zr_x$ alloys by mechanical alloying



1993 J. Phys.: Condens. Matter 5 477

(http://iopscience.iop.org/0953-8984/5/4/015)

J. Phys.: Condens. Matter 5 (1993) 477–484. Printed in the UK

# Synthesis and stability of amorphous $Cu_{60}Ti_{40-x}Zr_x$ alloys by mechanical alloying

Zhang Hen†‡, Liu Shaojun§, Su Yuchang‡§, Wang Lingling‡, Wu Lijun‡, Tan Zhaosheng‡ and Zhang Bangwei†‡

† CCAST (World Laboratory), PO Box 8730, Beijing 100080, People's Republic of China
‡ Department of Physics, Material Test and Research Centre, Hunan University, Changsha 410012, People's Republic of China
§ Department of Mechanical Engineering, Central-South University of Technology, Changsha 410013, People's Republic of China

Received 30 June 1992, in final form 23 September 1992

**Abstract.** The amorphous $Cu_{60}Ti_{40-x}Zr_x$ ($x = 0$, 10, 20 and 30) alloys were successfully synthesized by mechanical alloying of pure elemental powders of Cu, Ti and Zr using a planetary high-energy ball mill. The structure and thermal behaviour of these alloys were analysed by x-ray diffraction and differential scanning calorimetry. The results indicate that the replacement of Ti by Zr increases the chemical driving force of the amorphization reaction and the interaction of dissimilar atoms of the Cu–Ti–Zr ternary system. Thus, the glass-forming tendency, the amorphization rate and the stability are all improved. In addition, the stability of Cu–Ti–Zr amorphous powders is related to the crystallization sequence and the first crystallization phase.

## 1. Introduction

Amorphization by mechanical alloying (MA) has received much attention since 1983 when the first report of the Ni–Nb system [1] appeared. A large number of alloy systems has been investigated starting from elemental crystalline powders, showing that successful amorphization is generally possible in the central composition range of the binary phase diagram [2, 3].

Solid state amorphization is thought to require the following criteria [3–5]:

(1) fast diffusivity of solute atoms, which gives a characteristic reaction time for the nucleation and growth of the amorphous phase which is shorter than that of the crystalline phase;

(2) a large negative heat of mixing in the amorphous alloy, providing the necessary driving force for the reaction.

Cu–Ti and Cu–Zr are both important and interesting binary systems; furthermore, they have a large negative heat of mixing [3, 6], and the small Cu atom is a fast diffuser. Therefore, entirely amorphous Cu–Ti and Cu–Zr alloys have been successfully produced [1, 7, 8].

In contrast with binary alloys, investigation of the MA of ternary systems has not been so extensive, especially the reaction mechanism and the role of the third element during amorphization. For extensive investigation of the formation of the amorphous

0953-8984/93/040477+08$07.50  

phase in the Cu–Ti and Cu–Zr systems, the Cu–Ti–Zr ternary system is perhaps a suitable choice. Recently, we first synthesized an amorphous $Cu_{60}Ti_{20}Zr_{20}$ alloy by MA and the preliminary investigation indicated that the replacement of Ti by Zr can enhance the amorphization rate [9], but the effect of different degrees of replacement on glass formation and stability has not been investigated systematically yet. In the present work, we report the synthesis of the amorphous phase of $Cu_{60}Ti_{40-x}Zr_x$ by MA using a planetary mill and analyse the factors influencing the amorphization rate, glass-forming trend and thermal stability of the system.

## 2. Experimental details

Pure elemental powders (−200 mesh) of copper, titanium and zirconium were mixed to give the desired average compositions of $Cu_{60}Ti_{40-x}Zr_x$ ($x$ = 0, 10, 20 and 30) and placed in a cylindrical steel vial of diameter 40 mm and 60 mm long. The MA was carried out in a planetary high-energy ball mill with a ball-to-powder weight ratio of 10 to 1. Hardened steel balls of 15 mm diameter were used in the MA.

The specimens milled for different times during the milling process were analysed by x-ray diffraction (XRD) using a Siemens D-5000 diffractometer with Cu K$\alpha$ radiation. Accurate measurement at a scanning rate of 0.125° $min^{-1}$ was used to determine the position and the width of the half-height of the broad peaks (WHHP). The position of the peaks was determined using the chord method. The thermal behaviour was measured using a Dupont 1090 differential scanning calorimeter at a heating rate of 20 K $min^{-1}$ in flowing argon. In order to study the crystallization process and products, the amorphous powders were isothermally annealed at distinct temperatures corresponding to the exothermic peaks in the differential scanning calorimetry (DSC) curves; then the structures of the annealed powders were analysed by XRD.

## 3. Results and discussion

### *3.1. The formation of the amorphous phase*

Figure 1 shows a series of XRD patterns taken at 4 h intervals during the milling of $Cu_{60}Ti_{40-x}Zr_x$ starting from the elemental powder mixture. For all systems, after milling for 4 h all crystalline peaks markedly broaden and decrease in intensity. After milling for 8 h, a broad scattering maximum appears near $2\theta \equiv 42$–$43°$. The crystalline peaks have completely vanished after milling for 12 h. Apparently, the powders milled for 16 h have transformed to a completely amorphous phase. The analysis of the position of the amorphous diffraction peak by accurate XRD scanning indicates that typical amorphous XRD patterns with a broad scattering maximum appear near $2\theta$ = 43.00°, 42.80°, 42.60° and 42.28° for $Cu_{60}Ti_{40}$, $Cu_{60}Ti_{30}Zr_{10}$, $Cu_{60}Ti_{20}Zr_{20}$ and $Cu_{60}Ti_{10}Zr_{30}$, respectively, and the wavenumbers of the broad amorphous maximum are 2.99 $Å^{-1}$, 2.98 $Å^{-1}$, 2.96 $Å^{-1}$ and 2.94 $Å^{-1}$, respectively. Obviously, the wavenumber decreases with increasing zirconium content. The shift in the primary maximum can be attributed to a progressive increase in the near-neighbour distance with the partial replacement of Ti by Zr, because the metallic

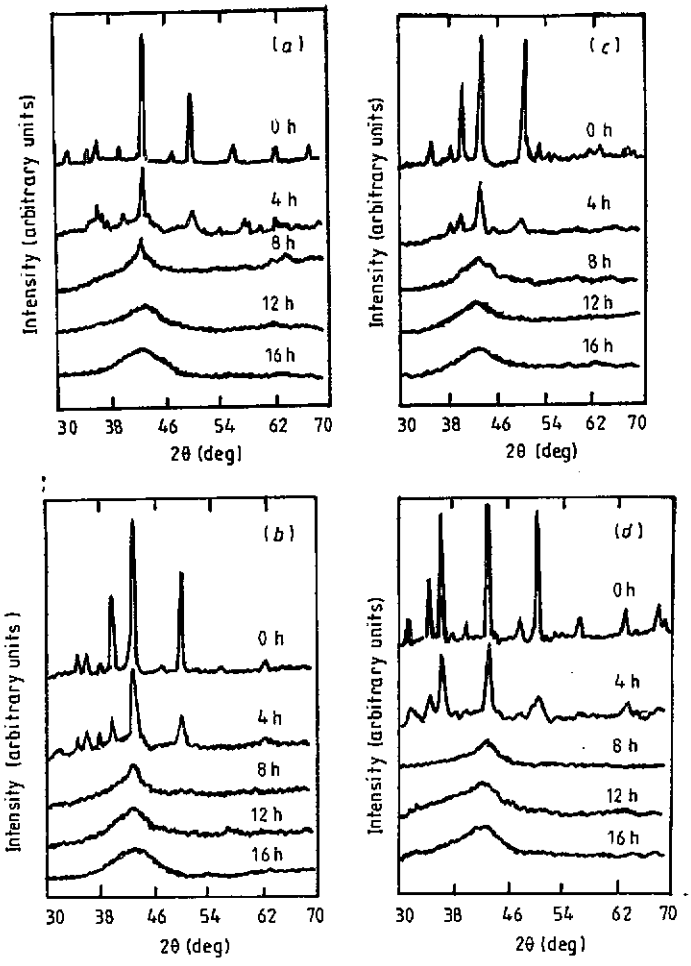


**Figure 1.** XRD patterns for (*a*) $Cu_{60}Ti_{40}$, (*b*) $Cu_{60}Ti_{30}Zr_{10}$, (*c*) $Cu_{60}Ti_{20}Zr_{20}$ and (*d*) $Cu_{60}Ti_{10}Zr_{30}$ after different milling times.

radii of Cu, Ti and Zr are $r_{Cu} = 1.28$ Å, $r_{Ti} = 1.47$ Å and $r_{Zr} = 1.60$ Å [10], and the radius of Zr is larger than that of Ti.

The XRD result indicates that the amorphization process takes place mainly during the milling period between 4 and 12 h and that, after 16 h, the four systems consist entirely of the amorphous phase. However, if we carefully analyse the XRD patterns after milling for 8 h, we may find that there are some differences between the WHHPs and shapes for the broad maximum. The WHHPs are 1.97°, 2.07°, 2.24°, and 2.17° for $Cu_{60}Ti_{40}$, $Cu_{60}Ti_{30}Zr_{10}$, $Cu_{60}Ti_{20}Zr_{20}$ and $Cu_{60}Ti_{10}Zr_{30}$, respectively. Furthermore, the shape of the broad peak of the Cu–Ti–Zr systems is smoother than that of $Cu_{60}Ti_{40}Zr_{40}$. These parameters can be used as an estimate of the degree of amorphization. Hence, this means that the degree and rate of amorphization are not the same for different zirconium contents. To analyse this difference, it is necessary to consider the chemical driving force which governs the diffusion reaction.

According to the work of Vijg [11], upon the addition of a third element to a binary alloy, an atomic–electronic interaction can result in a local rearrangement of

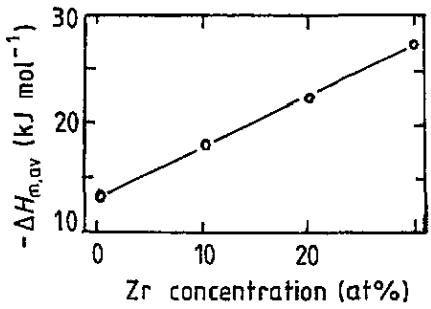


**Figure 2.** The enthalpy $\Delta\overline{H}_{m,av}$ of dissolution in liquid for $Cu_{60}Ti_{40-x}Zr_x$ alloys versus the zirconium concentration.

the atoms and the net effect can be expressed in terms of the enthalpy of solution of the element added to a liquid alloy [12]. The degree of interaction of dissimilar atoms by adding the third element of a ternary system can be evaluated from the enthalpy $\Delta\overline{H}_{m,av}$ of the third element in liquid binary alloys [13]. The enthalpy $\Delta\overline{H}_{m,av}$ can be expressed as

$$\Delta\overline{H}_{m,av} = X_{Ti}\,\Delta H^0_{Cu\text{ in }Ti} + X_{Zr}\,\Delta H^0_{Cu\text{ in }Zr} \tag{1}$$

where $X_i$ is the atomic fraction of element i (i ≡ Ti, Zr); $\Delta H^0_{Cu\text{ in }i}$ is the partial molar heat of solution in copper in liquid i (i ≡ Ti, Zr) at infinite dilution, which was calculated from the model of Miedema [12]. The relation between the enthalpy of dissolution and zirconium concentration for the $Cu_{60}Ti_{40-x}Zr_x$ alloys is presented in figure 2. This shows that the enthalpy of dissolution for the alloys becomes more negative on adding zirconium.

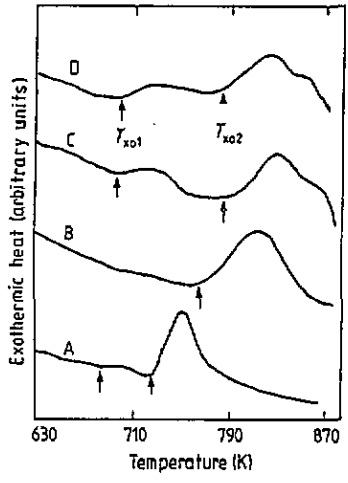


**Figure 3.** DSC traces for $Cu_{60}Ti_{40-x}Zr_x$ alloys milled for 16 h with $x = 0$ (curve A), $x = 10$ (curve B), $x = 20$ (curve C) and $x = 30$ (curve D). The onset crystallization temperatures are indicated by arrows.

The intensity of the Bragg reflection for the Cu–Ti and Cu–Ti–Zr systems decreases with increasing milling. This amorphization reaction type is indicated as the so-called type II by Weeber and Bakker [3]. The situation for reaction type II is that amorphization occurs by interdiffusion during the process. In this case the amorphization process is similar to amorphization of multilayered structures during heating [4]. The amorphization parts grow by cold welding of the amorphous layers formed by interdiffusion. Eventual homogenization takes place by adding Zr to the Cu–Ti system which would affect the above amorphization process. The powder sizes and properties (such as particle hardness), deformation and cold welding for the powders during the milling are not changed basically because the same alloy system and the same milling equipment are used. The main effect due to adding Zr to the system therefore is to affect the thermodynamic characteristics and interdiffusion of the system. Obviously there is basically no diffusion due to the concentration gradient, and the driving force for interdiffusion is caused by the chemical potential. The change in the Gibbs free energy caused by the change in entropy can be ignored, because of the lower milling temperature; so the change in the free energy, i.e. the change in the chemical potential, can be presented as the change in enthalpy. Figure 2 shows that $\Delta H$ increases on adding zirconium, which means that the chemical potential increases on adding zirconium; therefore the interdiffusion increases on adding zirconium. The fact that the degree and rate of amorphization increase on adding zirconium to the Cu–Ti system can now be understood qualitatively at least.

It is interesting to note that the increasing trends for both $\Delta H$ and the WHHP after milling for 8 h are similar on increase in the zirconium content. On the other hand, from a thermodynamic viewpoint, adding Zr increases the interaction of different kinds of atom, which leads to a more stable alloy configuration; obviously it is favourable for the formation of amorphous alloys. In other words, adding Zr increases the glass-forming tendency.

### *3.2. The thermal stability of amorphous powders*

The crystallization and thermal stability of the amorphous alloys were measured by DSC. Typical DSC curves for $Cu_{60}Ti_{40-x}Zr_x$ alloys milled for 16 h at a heating rate of 20 K $min^{-1}$ are presented in figure 3. The DSC trace of $Cu_{60}Ti_{40}$ shows a very weak broad peak at 710 K and a sharp exothermic peak at 757 K, which is similar to the result for liquid quenching [14, 15], but the exothermic peaks shift to a higher temperature and become broader. For $Cu_{60}Ti_{30}Zr_{10}$, only one exothermic peak can be observed at 822.1 K. Two exothermic peaks appear at 734.5 and 837.7 K for $Cu_{60}Ti_{20}Zr_{20}$ and at 734.5 and 828.2 K for $Cu_{60}Ti_{10}Zr_{30}$; the first exothermic peak is also broad and weak, and the other is stronger.

In the present work, we take the onset crystallization temperature $T_{xo}$, which is shown in table 1, as the criterion for estimating the stability of amorphous alloys. The data show that the stability of the amorphous alloys tends to increase as the zirconium concentration increases except for $Cu_{60}Ti_{30}Zr_{10}$, which has $T_{xo2}$ but no $T_{xo1}$ present in the DSC trace.

It was reported that the glass formation temperature for metallic glasses increases with increase in the cohesive energy of the glasses [16]. As a rough estimate, the cohesive energy can be represented by the heat of sublimation of elements. Accordingly the addition of an element with a higher heat of sublimation to the base metal would be expected to increase $T_g$ and hence the crystallization temperature

**Table 1.** Onset crystallization temperature $T_{xo}$ of amorphous $Cu_{60}Ti_{40-x}Zr_x$ alloys at a heating rate of 20 K $min^{-1}$.

| Zr (at.%) | $T_{xo1}$ (K) | $T_{xo2}$ (K) |
|---|---|---|
| 0 | 693.2 | 733.2 |
| 10 | — | 778.2 |
| 20 | 703.2 | 787.2 |
| 30 | 708.5 | 787.2 |

$T_c$ [17]. The sublimation enthalpies $\Delta H_s$ of Ti and Zr are 469.3 kJ $mol^{-1}$ and 612.1 kJ $mol^{-1}$ [18], respectively. Hence, with the replacement of Ti by Zr, we can infer that the sublimation enthalpy of the alloys will increase; thus, the stability of the glass will be improved. The results of the present work are similar to those on liquid-quenched Cu–Ti–Zr alloys, with the replacement of Ti by Zr; both the glass transition temperature $T_g$ and the crystallization temperature $T_c$ increase [19].

It can be considered that the deviation from the trend of stability versus Zr content for $Cu_{60}Ti_{30}Zr_{10}$ is due to a different crystallization process. As reported in [20], in some cases, structure changes in as-crystallized phases exert a strong effect on the temperature at the first crystallization peak $T_c$. If some compound was formed as the first phase and precipitated, both the stability and the glass-forming ability will be changed [21]. According to our preliminary XRD analysis for amorphous powders isothermally annealed to 500 and 600 °C for 2 h, we find that the first crystallization products and sequences are different (figure 4). With reference to the XRD measurement result, the data from ASTM standard cards and information about the Cu–Ti–Zr ternary phase diagram [22], we can roughly describe the crystallization sequence of amorphous $Cu_{60}Ti_{40-x}Zr_x$ alloys as follows:

$$\text{a-}Cu_{60}Ti_{40} \rightarrow Cu_3Ti \rightarrow Cu_3Ti + Cu_3Ti_2$$
$$\text{a-}Cu_{60}Ti_{30}Zr_{10} \rightarrow Cu_3Ti_2 \rightarrow Cu_3TiZr + Cu_3Ti_2 + Cu_3Ti$$
$$\text{a-}Cu_{60}Ti_{20}Zr_{20} \rightarrow Cu_2TiZr \rightarrow Cu_2TiZr + Cu_xTi_y + Cu_wZr_z$$
$$\text{a-}Cu_{60}Ti_{10}Zr_{30} \rightarrow Cu_2TiZr \rightarrow Cu_2TiZr + Cu_xZr_y + Cu_wZr_z$$

where $x$, $y$, $w$ and $z$ are values to be determined by further work.

From the above information, we can see that the first crystallization phase for $Cu_{60}Ti_{30}Zr_{10}$ is different from those for the other two Cu–Ti–Zr alloys. We can infer that the $Cu_3Ti_2$ phase may form at a higher temperature than the ternary $Cu_2TiZr$ phase does. This behaviour is, perhaps, one of the factors influencing the stability of amorphous alloys, but detailed research into the crystallization phase corresponding to every exothermic process is needed by combining transmission electron microscopy analysis and other methods with XRD in order to understand the stability of the amorphous alloys.

## 4. Conclusions

It is possible to produce amorphous $Cu_{60}Ti_{40-x}Zr_x$ alloys by MA. The replacement of Ti by Zr can enhance the amorphization rate of the Cu–Ti–Zr ternary system, promote the glass-forming tendency and improve the stability. These may be attributed to a

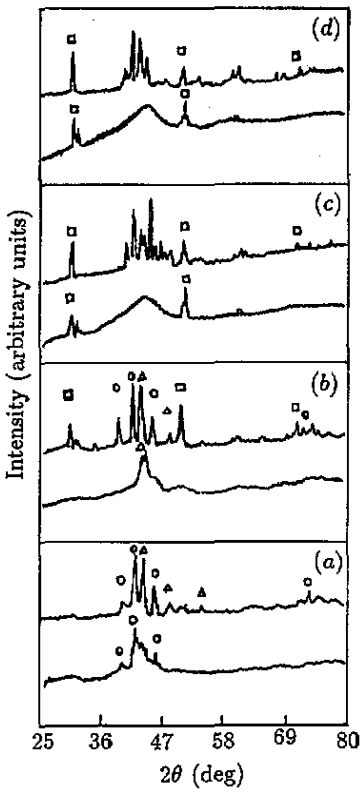


**Figure 4.** XRD patterns for amorphous $Cu_{60}Ti_{40-x}Zr_x$ powders isothermally annealed at 773 K (lower curves) and 873 K (upper curves) for 2 h with (*a*) $x = 30$, (*b*) $x = 20$, (*c*) $x = 10$ and (*d*) $x = 0$. ○, $Cu_3Ti$; △, $Cu_3Ti_2$; □, $Cu_2TiZr$.

more negative mixing enthalpy by adding zirconium to the Cu–Ti system, providing a larger chemical driving force of solid state reaction. On the other hand, adding zirconium to the Cu–Ti system strengthens the interaction of dissimilar kinds of atom in the ternary system, which leads to a more stable alloy configuration. Thus, the glass-forming ability and stability are simultaneously improved. However, the stability of amorphous powders is also related to the crystallization sequence, especially the behaviour of the first crystallization phase.

## References

[1] Koch C C, Cavin D B, McKancy C G and Scarbrough J O 1983 *Appl. Phys. Lett.* **43** 1017
[2] Eckert J, Schultz L and Urban K 1988 *J. Less-Common Met.* **145** 283
[3] Weeber A W and Bakker H 1988 *Physica* B **153** 92
[4] Schwarz R B and Johnson W L 1983 *Phys. Lett.* **51** 415
[5] Yeh X L, Samwer K and Johnson W L 1983 *Appl. Phys. Lett.* **42** 242
[6] Weeber A W and Bakker H 1988 *Z. Phys. Chem, NF* **157** 221
[7] Poltis C and Johnson W L 1986 *J. Appl. Phys.* **60** 1147
[8] Hellstern E and Schultz L 1988 *Z. Phys. Chem, NF* **157** 215
[9] Zhang H and Naugle D G 1992 *Appl. Phys. Lett.* **60** 2738
[10] Smithells C J and Brandes E A (ed) 1976 *Metals Reference Book* (London: Butterworths) p 100
[11] Vijg A K 1986 *J. Mater. Sci. Lett.* **5** 19
[12] Miedema A R, Boer F R and Boon R 1977 *Calphad* **1** 341
[13] Ghosh G, Chandarasekaran M and Delaey L 1991 *Acta Metall. Mater.* **39** 37
[14] Miao W F, Wang J, Li S L and Ding B I 1990 *J. Non-Cryst. Solids* **117–18** 230

[15] Marshall A F, Lee Y S and Stevenson D A 1983 *Acta Metall.* **31** 1225
[16] Chen H S 1974 *Acta Metall.* **22** 897
[17] Uhlmann D R 1977 *J. Non-Cryst. Solids* **25** 42
[18] Brandes E A (ed) 1983 *Smithells' Metals Reference Book* (London: Butterworths) p 18-2
[19] Massalski T B, Woychik C G and Dutkiewicz J 1988 *Metall. Trans.* A **19** 1853
[20] Lasocka M and Matyja H 1978 *Rapidly Quenched Metals III* ed B Cantor (London: Metals Society) p 339
[21] Zhao J J and Sekka Z 1987 *J. Non-Cryst. Solids* **88** 493
[22] Woychik G and Massalski B 1988 *Z. Metallk.* **79** 149